The Endosome-associated Deubiquitinating Enzyme USP8 Regulates BACE1 Enzyme Ubiquitination and Degradation*

Eniola Funmilayo Aduke Yeates[1] **and Giuseppina Tesco**[2]

From the Department of Neuroscience, Tufts University School of Medicine, Boston, Massachusetts 02111

The β-site amyloid precursor protein-cleaving enzyme (BACE1) is the rate-limiting enzyme in the production of amyloid-β, the toxic peptide that accumulates in the brain of subjects affected by Alzheimer disease. Our previous studies have shown that BACE1 is degraded via the lysosomal pathway and that that depletion of the trafficking molecule Golgi-localized γ-ear-containing ARF-binding protein 3 (GGA3) results in increased BACE1 levels and activity because of impaired lysosomal degradation. We also determined that GGA3 regulation of BACE1 levels requires its ability to bind ubiquitin. Accordingly, we reported that BACE1 is ubiquitinated at lysine 501 and that lack of ubiquitination at lysine 501 produces BACE1 stabilization. Ubiquitin conjugation is a reversible process mediated by deubiquitinating enzymes. The ubiquitin-specific peptidase 8 (USP8), an endosome-associated deubiquitinating enzyme, regulates the ubiquitination, trafficking, and lysosomal degradation of several plasma membrane proteins. Here, we report that RNAi-mediated depletion of USP8 reduced levels of both ectopically expressed and endogenous BACE1 in H4 human neuroglioma cells. Moreover, USP8 depletion increased BACE1 ubiquitination, promoted BACE1 accumulation in the early endosomes and late endosomes/lysosomes, and decreased levels of BACE1 in the recycling endosomes. We also found that decreased BACE1 protein levels were accompanied by a decrease in BACE1-mediated amyloid precursor protein cleavage and amyloid-β levels. Our findings demonstrate that USP8 plays a key role in the trafficking and degradation of BACE1 by deubiquitinating lysine 501. These studies suggest that therapies able to accelerate BACE1 degradation (*e.g.* by increasing BACE1 ubiquitination) may represent a potential treatment for Alzheimer disease.

Alzheimer disease (AD)[3] is a progressive neurodegenerative disorder characterized by memory impairments and cognitive deterioration. AD is characterized by the cerebral accumulation of amyloid-β (Aβ), a 4-kDa peptide formed by the serial proteolysis of amyloid precursor protein (APP), by the β- and γ-secretases. The β-secretase responsible for APP cleavage has been identified as BACE1, a membrane-tethered aspartyl protease (1–4). APP more commonly undergoes non-amyloidogenic processing by α-secretases that cleave APP in the middle of the β-amyloid domain (5). Candidate α-secretases include ADAM9 (A disintegrin and metalloproteinase domain-containing protein), ADAM10, and ADAM17, also known as tumor necrosis factor-α converting enzyme (6, 7). The γ-secretase activity requires a set of four proteins, including presenilin 1 and 2, nicastrin, anterior pharynx defective 1 (APH1), and presenilin enhancer 2 (PEN-2) (8). Presenilins are aspartyl proteases and are the catalytic subunit of the γ-secretase complex. APP proteolysis by β- and α-secretases results in the production of secreted APP polypeptides along with membrane-associated APP-C-terminal fragments (APP-CTFs) C99 and C89 (generated by β-secretase) and C83 (generated by α-secretase). APP-CTFs can then serve as substrates for γ-secretase resulting in the production of Aβ (C99-C89) or p3 (C83) and the APP intracellular domain (AICD) (9).

BACE1 is an *N*-glycosylated type 1 transmembrane protein that undergoes constitutive N-terminal processing in the Golgi apparatus. The ectodomain contains four glycosylation sites and two signature sequences typically associated with aspartyl proteases (D(T/S)G(T/S)) (10). BACE1 is targeted through the secretory pathway to the plasma membrane where it is internalized to the endosomes and subsequently trafficked back to the cell surface or trans-Golgi network through recycling endosomes or transported to the lysosomes for degradation (11). Sorting of membrane proteins to the endosomes and lysosomes is regulated by the interaction of signals present in the C-terminal fragment (CTF) with specific trafficking molecules (12). Our previous studies have shown that BACE1 is degraded via the lysosomal pathway (13) and that depletion of the trafficking molecule Golgi-localized γ-ear-containing ARF-binding protein 3 (GGA3) results in increased BACE1 levels and activity (14, 15). We also determined that GGA3 regulation of BACE1 levels requires its ability to bind ubiquitin (Ub). Accordingly, we reported that BACE1 is ubiquitinated at lysine 501 (16) and that lack of ubiquitination at Lys-501 produces BACE1 stabilization (17).

[3] The abbreviations used are: AD, Alzheimer disease; AICD, APP intracellular domain; APP, amyloid precursor protein; Aβ, amyloid-β; BACE1, β-site amyloid precursor protein-cleaving enzyme; CTF, C-terminal fragment; EGFR, epidermal growth factor receptor; ESCRT, endosomal sorting complex required for transport; HRS, hepatocyte growth factor-regulated tyrosine kinase substrate; MVB, multivesicular body; NEM, *N*-ethylmaleimide; NT, non-targeting; RIPA, radioimmunoprecipitation assay; STAM, signal transducing adaptor molecule; Ub, ubiquitin; Tricine, *N*-[2-hydroxy-1,1-bis(hydroxymethyl)ethyl]glycine; BisTris, 2-[bis(2-hydroxyethyl)amino]-2-(hydroxymethyl)propane-1,3-diol; ANOVA, analysis of variance; STAM, signal transducing adaptor molecule.

USP8 Depletion Decreases BACE1 and Aβ Levels

Ubiquitin, a tag for protein degradation, is covalently attached to the ε-amino group of lysine residues in the target protein by a cascade of reactions involving at least three enzymatic activities as follows: E1, E2, and E3 ligases. Originally, ubiquitination was thought to solely tag proteins for proteasomal degradation. However, it is now well established that ubiquitin is a sorting signal for membrane proteins at the trans-Golgi network, plasma membrane, and endosomes to be delivered to lysosomes (18). The specificity and outcomes of ubiquitin signaling depend on the number of ubiquitin molecules (mono- or poly-ubiquitination) and the type of poly-ubiquitin chain attached to the substrate (19). Elongation of polyUb chains can occur at any of the seven lysines present in ubiquitin. Lys-48-linked ubiquitination mainly targets proteins for proteasomal degradation. In contrast, increasing evidence suggests that Lys-63-linked Ub chains are a specific signal for protein sorting into the multivesicular body (MVB) pathway (20). Accordingly, we have determined that BACE1 is mainly mono- and Lys-63-linked poly-ubiquitinated, suggesting a role for ubiquitination in sorting BACE1 to the lysosomes for degradation (17).

Ubiquitin conjugation is a reversible process mediated by deubiquitinating enzymes (DUBs). The human genome encodes ~95 putative DUBs. These DUBs are either zinc-dependent metalloproteases or cysteine proteases (21). Ubiquitin-specific peptidase 8 (USP8) is a member of the DUB family of cysteine proteases that is expressed throughout the brain. Its highest expression is in the CA1 and dentate gyrus of the hippocampus, as well as the preoptic nucleus and the paraventricular nucleus in the diencephalon (22). Within the cell, USP8 has been found in the cytoplasm and at the endosome (23–25). USP8 degrades Lys-48-, Lys-63-, and Lys-6-linked ubiquitin chains (26, 27). USP8 has been shown to negatively regulate the ubiquitination of lysosome-degraded proteins, including the epidermal growth factor receptor (EGFR) (23, 28, 29); tropomyosin-related kinase A (TRKA) (25); AMPA receptor (30); vascular endothelial growth factor receptor 2 (VEGFR2) (31); leucine-rich repeats and immunoglobulin-like domains 1 (LRIG1) (32); potassium intermediate/small conductance calcium-activated channel, subfamily N, member 4 (KCA3.1) (33); protease-activated receptor 2 (PAR2) (34); and δ-opioid receptor (35).

The effect of USP8 on EGFR has been widely studied. Although some investigators have noted an increase in total cellular EGFR when USP8 is depleted (24, 28), others have determined that USP8 depletion leads to an increase in EGFR lysosomal degradation, accompanied by a decrease in EGFR protein levels in both cellular and mouse conditional knock-out models (23, 36, 37). USP8 has a role not only in protein degradation but also in protein trafficking. It has been shown that USP8 binds to the Src homology 3 domain of signal transducing adaptor molecule (STAM) (38) and stabilizes it (24). STAM is a component of the ESCRT0 complex. The ESCRT complexes are important components of the endosomal-lysosomal machinery. Ubiquitinated cargoes are passed sequentially from ESCRT0 to ESCRT-I to ESCRT-II and then finally deposited into the forming luminal vesicles (18). ESCRT0, comprising HRS (hepatocyte growth factor-regulated tyrosine kinase substrate) and STAM, aids in the docking of ubiquiti-

nated proteins to the endosomes (40). As USP8 stabilizes STAM, USP8 may play a role in facilitating the passage of molecules destined for degradation along the endosome-lysosome degradation pathway. Notably, USP8 depletion or overexpression of catalytically inactive USP8 leads to the accumulation of ubiquitinated proteins in the endosomes (24, 34, 36, 41).

Here, we report that RNAi-mediated knockdown of USP8 results in a decrease in BACE1 protein levels because of increased BACE1 ubiquitination and degradation in human H4 neuroglioma cells. As a consequence, BACE1-mediated APP cleavage and amyloid-β formation are also decreased in USP8-depleted cells. Our findings suggest that therapies able to accelerate BACE1 degradation (*e.g.* by increasing BACE1 ubiquitination) may represent a potential treatment for AD.

Results

USP8 Depletion Decreases BACE1-GFP but Not ADAM10 and Presenilin 1 Protein Levels—Depletion of USP8 has been shown to decrease protein levels of USP8 substrates, as a result of increased substrate ubiquitination and degradation (23, 36). To determine whether USP8 depletion resulted in a decrease in BACE1, we performed siRNA-mediated knockdown of USP8, using two different siRNAs targeting USP8 in an H4 neuroglioma cell line overexpressing BACE1-GFP (H4-BACE1-GFP). Treatment of cells with USP8 siRNA#3 and USP8 siRNA#2 resulted in an 87 ± 7 and 85 ± 5% reduction of USP8 protein levels, respectively, compared with NT siRNA-treated cells (mean ± S.E., $p < 0.0001$; one-way ANOVA, and Tukey's multiple comparison test, $n = 3$ independent experiments). Knockdown with each siRNA resulted in an independent decrease in BACE1-GFP protein in H4-BACE1-GFP cells ($p = <0.05$; one-way ANOVA and Tukey's multiple comparison test, $n = 4$ independent experiments) (Fig. 1, *A* and *B*). Furthermore, to determine whether this protein decrease was specific for BACE1, we examined the protein levels of two other proteins important in APP processing, ADAM10, the prevalent α-secretase of APP, and presenilin 1 (PS1), the catalytic subunit of the γ-secretase complex. USP8 depletion did not result in any change in ADAM10 or PS1 protein levels (Fig. 1, *C–E*) (the p value >0.05 indicates that the difference is not significant; one-way ANOVA and Tukey's multiple comparison test, $n = 3$ independent experiments). The decrease in BACE1 protein but not ADAM10 or PS1 indicated that the effect of USP8 depletion is specific to BACE1 and not to other enzymes that also cleave APP.

USP8 Depletion Decreases Endogenous BACE1 Protein Levels—Next, we determined whether USP8 depletion resulted in a similar decrease in endogenous BACE1. USP8 was knocked down in H4 cells, which express endogenous levels of BACE1. Initial trials using a concentration of 25 nM siRNA with this cell line resulted in toxicity. Thus, the siRNA concentration was reduced to 5 nM, and treatment time was reduced to 48 h rather than 96 h. Western blotting analysis of lysates obtained from USP8-depleted or NT siRNA-treated cells revealed a decrease in USP8 accompanied by a decrease in endogenous BACE1 ($p = 0.0001$; unpaired t test with Welch's correction; $n = 4$ independent experiments) (Fig. 2, *A* and *B*). This demonstrated that
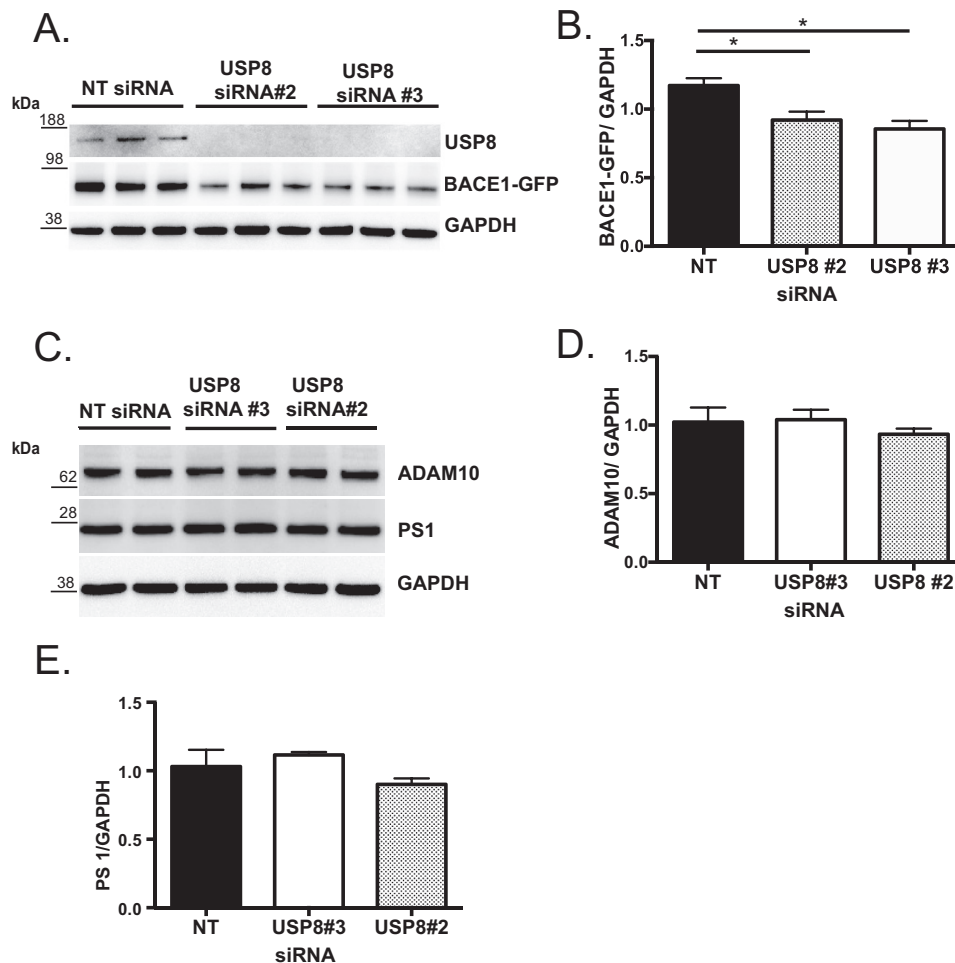
FIGURE 1. **USP8 depletion decreases BACE1-GFP but not ADAM10 and presenilin 1 protein levels.** *A,* representative Western blot showing decreased levels of BACE1-GFP in H4 neuroglioma-stable cell lines expressing BACE1-GFP depleted of USP8 by using two separate siRNAs (*#2* and *#3*). *B,* quantification of BACE1-GFP normalized to GAPDH. *C,* representative Western blot showing unchanged levels of ADAM10 and PS1 in H4 neuroglioma stable cell lines expressing BACE1-GFP depleted of USP8 by using two separate siRNAs (*#2* and *#3*). *D,* quantification of ADAM10 normalized to loading control, GAPDH. *E,* quantification of PS1 normalized to GAPDH. *Graphs* show mean and S.E. $n = 3$ independent experiments; *, $p < 0.05$; one-way ANOVA and Tukey's multiple comparison test. *NT,* non-targeting.

USP8 depletion resulted in a decrease in endogenous BACE1, similar to the observed decrease in BACE1-GFP.

Inhibition of Lysosomal Degradation Rescues USP8-dependent BACE1 Protein Decrease—As BACE1 is degraded in the lysosomes, we hypothesized that the decrease in BACE1 protein levels observed with USP8 depletion was due to increased degradation of BACE1 in the lysosomes. To determine whether lysosomal degradation was a possible mechanism for the decrease in BACE1 protein levels in USP8-depleted cells, we treated USP8-depleted and NT siRNA-transfected cells with chloroquine, a weak base, which inhibits lysosomal hydrolases. Chloroquine treatment resulted in an accumulation of BACE1-GFP in both USP8 and NT siRNA-treated samples (Fig. 3, *A* and *B*). Thus, lysosomal inhibition rescued the decrease of BACE1-GFP protein levels in USP8-depleted cells, indicating that USP8 regulates lysosomal degradation of BACE1.

USP8 Deubiquitinates BACE1 at Lysine 501—Depletion of USP8 results in an increase in the ubiquitination of its substrates (23, 24, 30–32, 36). Thus, we tested whether USP8 depletion would result in increased BACE1 ubiquitination. BACE1-GFP was immunoprecipitated with anti-GFP antibody

in lysates of cells treated with either USP8 or NT siRNA for 96 h. Western blotting analysis of immunoprecipitated BACE1-GFP using anti-Ub antibody revealed that BACE1-GFP was significantly more ubiquitinated in USP8-depleted than control samples (Fig. 4, *A* and *B*) ($p = 0.0003$; unpaired *t* test with Welch's correction; $n = 4$ independent experiments). We have previously shown that BACE1 is ubiquitinated at Lys-501 and that the K501R mutation prevents BACE1 ubiquitination (16, 17). Thus, we tested whether USP8 deubiquitinates BACE1 at Lys-501 by depleting USP8 in the H4-BACE1-K501R cell line. BACE1-GFP was immunoprecipitated from cell lysates using anti-GFP antibody. Western blotting analysis of immunoprecipitates with anti-Ub antibody revealed that BACE1-K501R GFP had negligible levels of ubiquitination. Furthermore, depletion of USP8 did not lead to the large increases in ubiquitination, observed in wild-type BACE1-GFP (Fig. 4*A*). These data indicate that USP8 is responsible for deubiquitinating BACE1 at Lys-501. However, indirect effects of USP8 could not be ruled out as the experiment was carried out in cells.

Thus, to determine whether USP8 directly deubiquitinated BACE1, a cell-free reaction was prepared. BACE1-GFP was
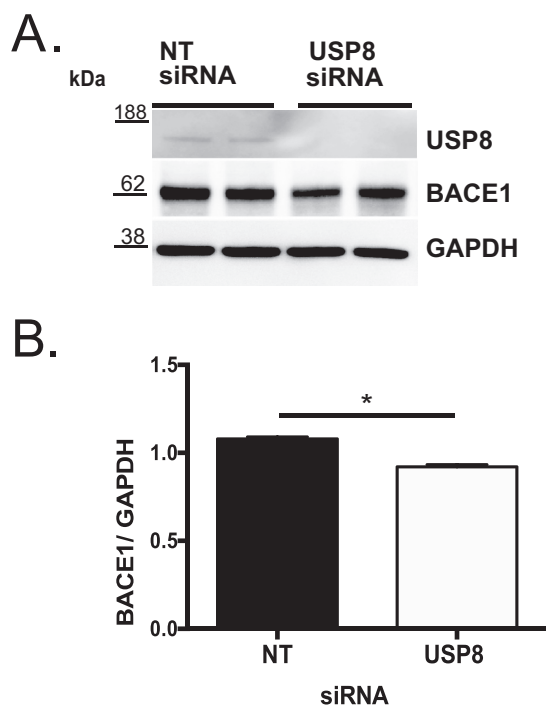
A.

B.

FIGURE 2. USP8 knockdown decreases endogenous BACE1 protein levels in H4 cells. Protein levels of endogenous BACE1 were evaluated in H4 cell lysates 48 h post-transfection. *A,* representative Western blot; *B,* quantification of BACE1 normalized to loading control, GAPDH. *Graph* shows mean and S.E.; $n = 4$ independent experiments; *, $p = 0.0001$; unpaired *t* test with Welch's correction. *NT,* non-targeting.
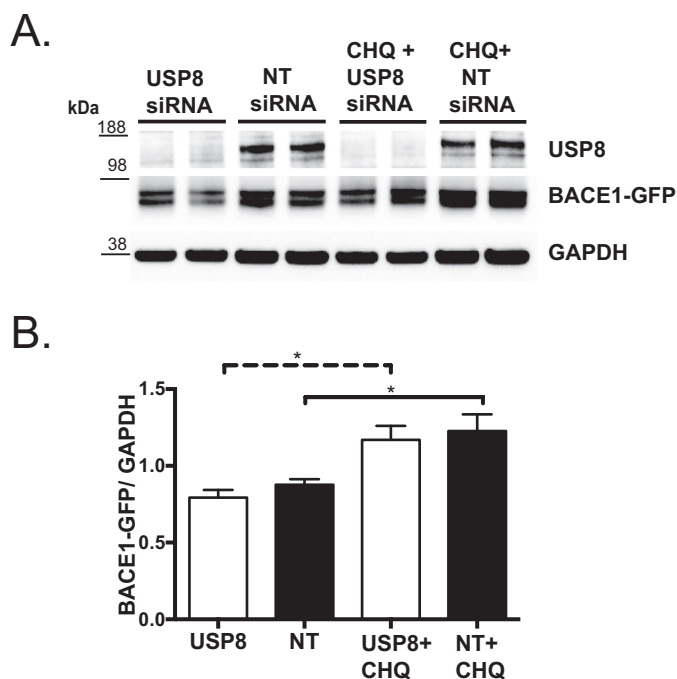
A.

B.

FIGURE 3. Inhibition of lysosomal degradation rescues USP8-dependent BACE1 protein decrease. Chloroquine (25 μM) treatment caused an accumulation of BACE1-GPF protein in both USP8 and NT siRNA-treated cells. *A,* Western blot; *B,* quantification of BACE1-GFP normalized to loading control, GAPDH. *Graph* shows mean and S.E.; $n = 5$ independent experiments; *, $p < 0.05$; one-way ANOVA and Tukey's multiple comparison test. *CHQ,* chloroquine; *NT,* non-targeting.

immunoprecipitated with anti-GFP antibody from USP8-depleted samples, where BACE1-GFP was highly ubiquitined. Immunoprecipitates immobilized on protein A/G plus-agarose beads were mixed with human recombinant FLAG-USP8 and incubated at 37 °C for 120 min. Furthermore, 5 mM NEM, a cysteine protease inhibitor, known to inhibit DUBs, was included as an experimental negative control in some samples. In this cell-free reaction, samples containing recombinant FLAG-USP8 had very low levels of ubiquitination after 120 min, compared with samples where no recombinant USP8 was included. Furthermore, addition of NEM with recombinant FLAG-USP8 inhibited the decrease in ubiquitination (Fig. 4C). These data indicate that USP8 directly deubiquitinates BACE1.

USP8 Depletion Results in BACE1 Accumulation in Early Endosomes and Lysosomes and Reduction in Recycling Endosomes—Lysine 63-linked polyubiquitination is a known signal for protein trafficking to the lysosomes. We have previously reported that BACE1 is degraded by the lysosomes and that it is lysine 63-linked polyubiquitinated (16, 17). As USP8 depletion resulted in an increase in BACE1 ubiquitination, we hypothesized that there would be a resultant increase in BACE1 trafficking to the endosomes and then to the lysosomes for degradation. Subcellular localization of BACE1-GFP was assessed in H4-BACE1-GFP cells 96 h post-transfection of USP8 or NT siRNA. To identify the different subcellular compartments, cells were immunostained with markers for early endosomes (EEA1), late endosomes/lysosomes (LAMP2), and recycling endosomes (RAB11). Confocal microscopy showed that BACE1-GFP percentage intensity was increased in EEA1-positive regions and in USP8-depleted compared with NT siRNA-treated cells ($p = 0.0025$, unpaired *t* test with Welch's correction) (Fig. 5, *A* and *B*). We also found an increase in the percentage intensity of BACE1-GFP in LAMP2-positive regions ($p < 0.0001$, unpaired *t* test with Welch's correction) (Fig. 5, *C* and *D*) in USP8-depleted cells. In contrast, we found a decrease in the percentage intensity of BACE1-GPF in RAB11-positive regions, when USP8 was depleted ($p = 0.0057$, unpaired *t* test with Welch's correction) (Fig. 5, *E* and *F*). These data suggest that USP8 regulates the trafficking of BACE1 after its internalization by favoring the recycling of BACE1, while negatively regulating its lysosomal degradation.

We also noted a 1.8-fold increase in the size of BACE1-positive puncta ($p < 0.0001$, unpaired *t* test with Welch's correction). Moreover, the size of EEA1-labeled endosomes and RAB11-positive recycling endosomes was increased by 1.5- and 1.8-fold, respectively ($p < 0.0001$, unpaired *t* test with Welch's correction). In contrast, there was no change in the size of the LAMP2-positive lysosomes ($p = 0.068$, unpaired *t* test with Welch's correction) (Fig. 5G). Our findings are in agreement with previous reports showing that depletion of USP8 or overexpression of a dominant negative USP8 mutant causes the accumulation of ubiquitinated proteins within endosomes and a corresponding increase in endosome size (24, 31, 34, 36, 41, 42).

USP8 Knockdown Decreases APP-C99 and C89 Generation in H4-BACE1-GFP Cells—As USP8 depletion resulted in a decrease in BACE1 protein levels, we next determined whether there would be an accompanying decrease in BACE1-mediated
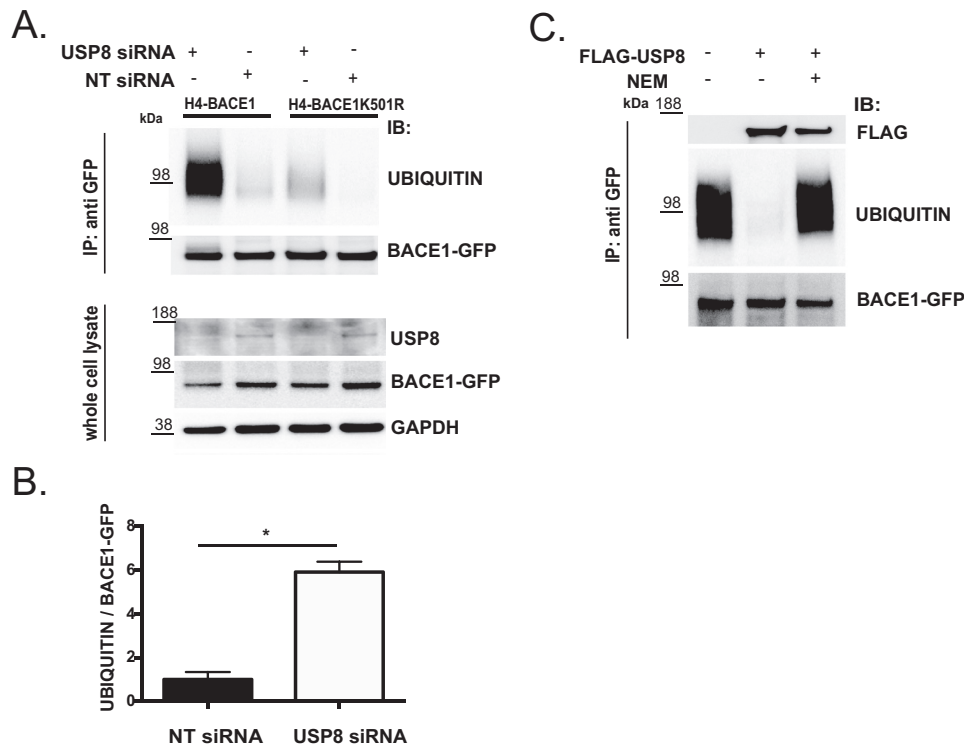
FIGURE 4. **USP8 deubiquitinates BACE1 at lysine 501.** *A,* USP8 depletion increases BACE1 ubiquitination. Ubiquitinated BACE1-GFP or BACE1-K501R was immunoprecipitated (*IP*) from cells treated with either USP8 or NT siRNA. USP8 depletion increased ubiquitination of immunoprecipitated BACE1. *B,* quantification of ubiquitin normalized to immunoprecipitated BACE1-GFP. *Graph* shows mean and S.E.; $n = 4$ independent experiments; *, $p = 0.0003$, unpaired *t* test with Welch's correction. *C,* USP8 deubiquitinates BACE1 in cell-free assay. Western blot showing ubiquitinated BACE1 after incubation with recombinant FLAG-USP8 in cell-free assay with or without 5 mM NEM for 120 min at 37 °C. *NT,* non-targeting; IB, immunoblot.

APP processing. BACE1 cleaves APP at two sites forming APP-C99 and -C89, whereas α-secretase generates APP-C83. These C-terminal fragments (CTF) may exist in non-phosphorylated and phosphorylated forms. Accordingly, five APP-CTFs may be resolved on Western blotting, corresponding to APP-CTFs pC99, C99, pC89, C89 + pC83, and C83 in H4 cells (Fig. 6A). However, three bands corresponding to pC99, pC89, C89 + pC83 were the most apparent in H4-BACE-GFP cell lysates because of increased β-secretase processing and were hence quantified (Fig. 6A).

Lysates from H4-BACE1-GFP cells treated with USP8 and NT siRNA were separated by SDS-PAGE using 16.5% Tris-Tricine gels (Bio-Rad) and incubated with C1/6.1 antibodies (Biolegend) to detect full-length APP and APP CTFs. USP8 depletion increased the amount of full-length APP (Fig. 6, *B* and *C*), which is consistent with decreased BACE1 processing. Furthermore, USP8 depletion decreased the ratio of pC99/APP and pC89/APP (Fig. 6, *D* and *E*). However, the ratio of C89 + pC83 to APP remained unchanged (Fig. 6F) ($p < 0.05$; unpaired *t* test with Welch's correction, $n = 6$ independent experiments). Given that pC99 and pC89 are products of BACE1-mediated APP cleavage, decreased protein levels of these APP-CTFs suggested a decrease in β-secretase processing of APP.

USP8 Depletion Decreases APP-C99 and C89 Generation in H4 Cells but Not APP-CTF Degradation—Because USP8 depletion resulted in a decrease in products of BACE1-mediated APP processing in H4-BACE1-GFP cells, we sought to determine whether a similar effect could be observed in H4 cells, with endogenous levels of BACE1. Lysates from H4 cells treated with
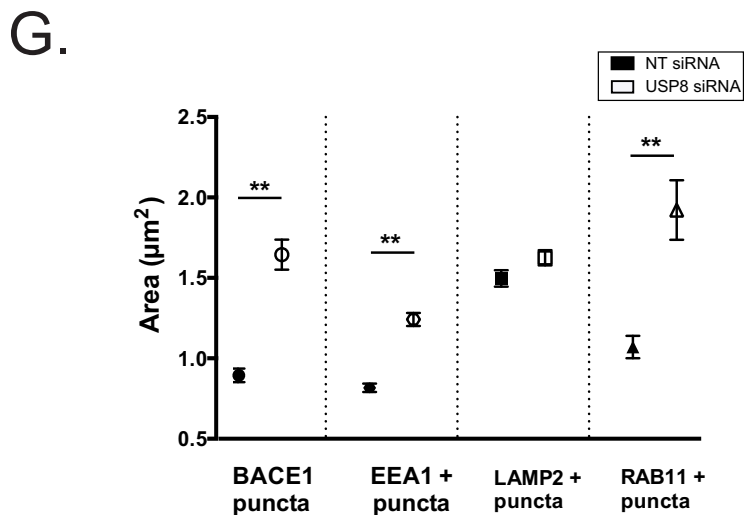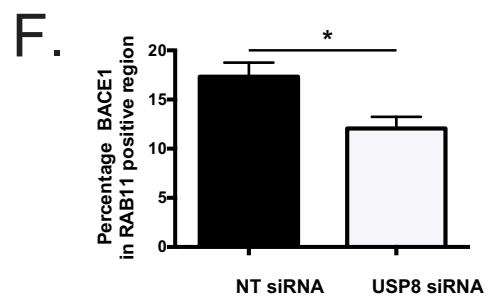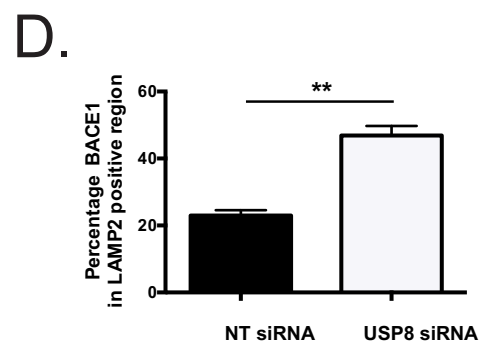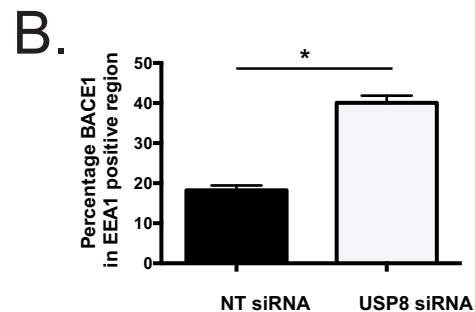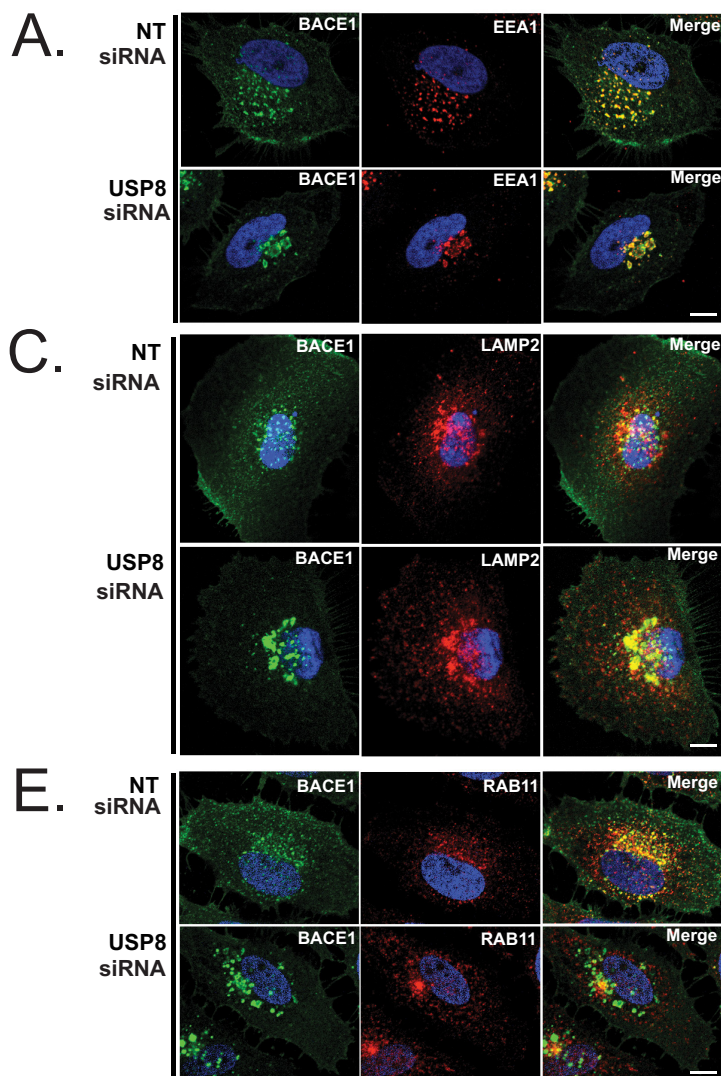
USP8 and NT siRNA were separated by SDS-PAGE using 16.5% Tris-Tricine gels and incubated with C1/6.1 antibody (Biolegend) to detect full-length APP and APP CTFs. Like in H4-BACE1-GFP cells, USP8 depletion led to a slight increase in the amount of full-length APP (Fig. 7, *A* and *B*). Furthermore, USP8 depletion decreased the ratio of pC99/APP, C99/APP, pC89/APP, and C89 + pC83/APP (Fig. 7, *C–F*). However, the C83/APP ratio remained unchanged (Fig. 7G) ($p < 0.05$; unpaired *t* test with Welch's correction, $n = 3–4$ independent experiments). These results demonstrated that the decrease in endogenous BACE1 with USP8 depletion (Fig. 2, *A* and *B*) was sufficient to decrease BACE1-mediated APP processing. Decreased protein levels of these APP-CTFs suggested a decrease in β-secretase processing of APP, because pC99, C99, and pC89 are products of BACE1-mediated APP cleavage.

APP-CTFs are ubiquitinated and degraded in the lysosomes (43); thus, a decrease in pC99, C99, and pC89 may also have arisen from increased APP-CTF degradation in a BACE1-independent manner. Thus, H4 cells overexpressing APP-C99 were transfected with either USP8 or NT siRNA. Western blotting analysis revealed that USP8 depletion did not alter the levels of overexpressed C99 ($p = 0.4561$; unpaired *t* test with Welch's correction; $n = 3$ independent experiments), indicating that USP8 depletion did not decrease APP-CTFs degradation in a BACE1-independent manner (Fig. 7, *H* and *I*). Altogether, these data indicate that the decrease in BACE1 observed with USP8 depletion leads to a decrease in BACE1-mediated APP processing.

USP8 Depletion Decreases BACE1 and Aβ Levels

USP8 Knockdown Decreases AICD Levels—γ-Secretase cleavage of APP-CTFs results in the production of Aβ (C99-C89) or p3 (C83) and AICD (9). It has been previously reported that NEM treatment of cultured cells stabilizes AICD (44). Given that NEM inhibits USP8 in a cell-free assay (Fig. 4), we sought to determine whether USP8 depletion affected the stability of AICD. Endogenous levels of AICD in H4 cell lysates are low and difficult to detect, and thus we overexpressed APP-C60 (45) in H4 cells.
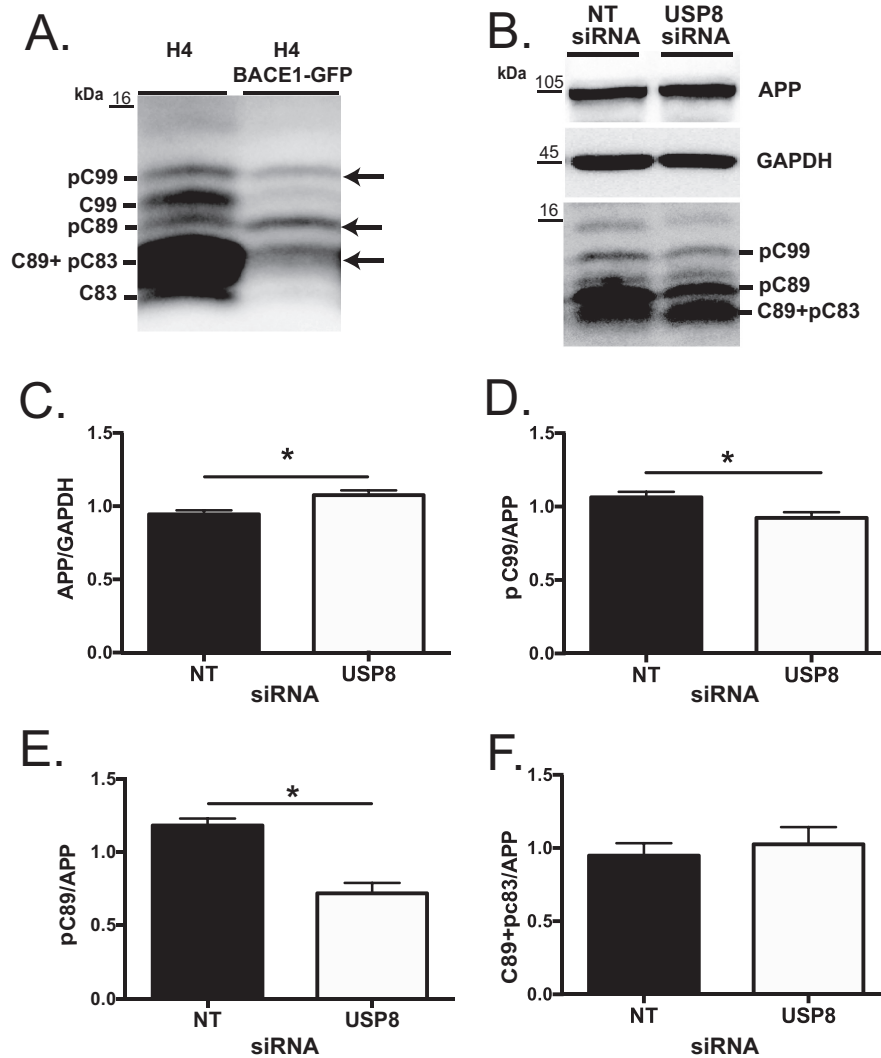
FIGURE 6. **USP8 depletion decreases APP-C99 and -C89 generation in H4-BACE-GFP cells.** USP8 knockdown decreases the ratio of pC99 and pC89 but not C89 + pC83 to full-length APP. *A,* representative Western blot showing prominent APP-CTF bands in untreated cell lysates. *B,* lysates from H4-BACE-GFP cells were separated by SDS-PAGE using 16.5% Tris-Tricine gels and incubated with C1/6.1 antibodies to label full-length APP and APP-C-terminal fragments. Representative Western blot. *C,* quantification of full-length APP normalized to GAPDH; *, $p = 0.0199$. *D,* ratio of pC99 to APP; *, $p = 0.0255$. *E,* ratio of pC89 to APP; *, $p = 0.0005$; *F,* ratio of C89 + pC83 to APP; $p = 0.602$. *Graphs* show mean and S.E.; $n = 6$ independent experiments; unpaired *t* test with Welch's correction. *NT,* non-targeting.

The APP-C60 plasmid expresses a protein containing the terminal 59 amino acid residues of APP, along with an initiating methionine residue. This sequence corresponds to the portion of the APP-CTF that occurs after the γ-secretase cleavage site at position 40 within Aβ (45). Overexpressing C60 allowed the effect of USP8 depletion on AICD levels to be measured independently of the changes in APP-CTF levels. USP8 depletion resulted in decreased C60 protein levels ($p = 0.0187$; unpaired *t* test with Welch's correction; $n = 3$ independent experiments), suggesting that USP8 may play a role in stabilizing the AICD

(Fig. 8). These data also indicate that NEM stabilizes AICD by inhibiting proteases other than USP8.

USP8 Depletion Decreases Aβ Production in H4 Cells—As there was a decrease in the ratio of pC99 and pC89 to full-length APP, we hypothesized that there would be a decrease in the level of Aβ production with USP8 depletion. Aβ(1–40) content was measured in conditioned media from H4-BACE1-GFP cells treated with USP8 or NT siRNA. However, depletion of USP8 did not result in a decrease of Aβ(1–40) in this cell line (data not shown). Given that the overexpression of BACE1 has

FIGURE 5. **USP8 depletion results in BACE1 accumulation in early endosomes and lysosomes and reduction in recycling endosomes.** *A,* representative photomicrograph of H4-BACE-GFP cell treated with NT or USP8 siRNA, labeled with early endosome marker EEA1. *B,* USP8 depletion increases the percentage of BACE1 in EEA1-positive regions. Percentage was derived by dividing total intensity of BACE1-GFP in EEA1-positive regions by total GFP intensity in the cell. *C,* representative photomicrograph of H4-BACE-GFP cell treated with NT or USP8 siRNA, labeled with late endosome/lysosome marker, LAMP2. *D,* USP8 depletion increases the percentage of BACE1 in LAMP2-positive regions. *E,* representative photomicrograph of H4-BACE-GFP cell treated with NT or USP8 siRNA, labeled with recycling endosome marker, RAB11. *F,* USP8 depletion decreases the percentage of BACE1 in RAB11-positive regions. *G,* USP8 depletion results in an increase in the area of BACE1-positive puncta, EEA1-positive early endosomes, and RAB11-positive recycling endosomes, but not LAMP2-positive lysosomes. Nuclei, shown in *blue,* are labeled with DAPI. *Graphs* show mean and S.E., $n = 43$–55 cells per condition, from three independent experiments. *, $p < 0.01$; **, $p < 0.0001$; unpaired *t* test with Welch's correction. *Scale bar,* 10 μm. *NT,* non-targeting.
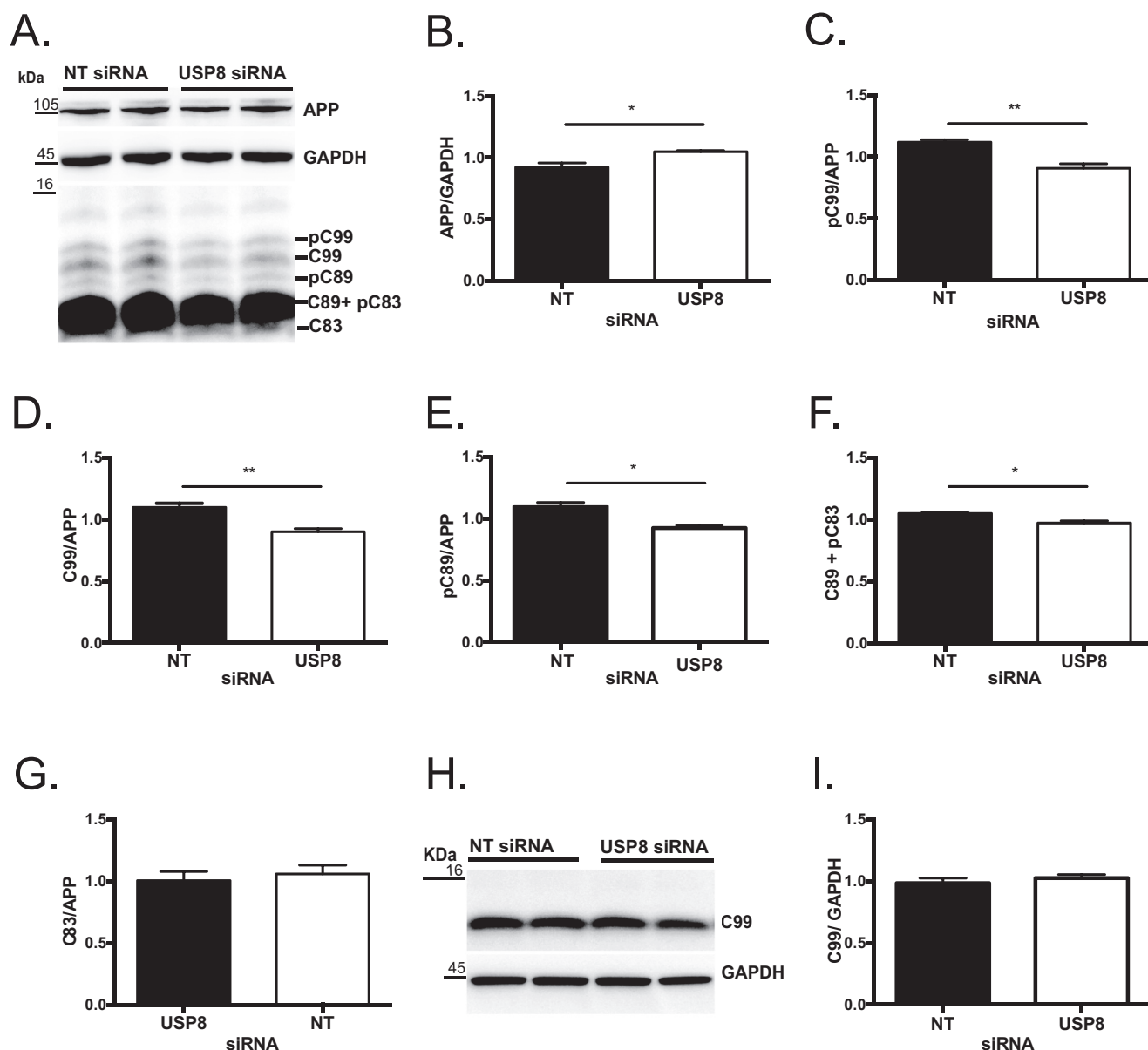
FIGURE 7. **USP8 depletion decreases APP-C99 and -C89 generation in H4 cells but not APP-CTF degradation.** USP8 knockdown decreases the ratio of pC99, C99, pC89, and C89 + pC83 to full-length APP but not C83. *A*, representative Western blot; *B*, quantification of full-length APP normalized to GAPDH; *, $p = 0.0315$. *C*, ratio of pC99 to APP; *, $p = 0.0049$. *D*, ratio of C99 to APP; *, $p = 0.0059$; *E*, ratio of pC89 to APP; *, $p = 0.0124$; *F*, ratio of C89 + pC83 to APP; *, $p = 0.0137$; *G*, ratio of C83 to APP; $p = 0.602$. USP8 depletion does not affect overexpressed C99 levels in H4-C99 cell line. *H*, representative Western blot; *I*, quantification of C99 normalized to GAPDH. Graphs show mean and S.E.; $n = 3–4$ independent experiments; unpaired *t* test with Welch's correction, *NT*, non-targeting.

been shown to promote APP processing at the β'-site resulting in the increased production of +11 Aβ species (4, 46, 47), it is possible that in H4-BACE1-GFP cells the decrease in BACE1 results in a reduction of +11Aβ, which is not detected by the ELISA. Accordingly, the levels of pC89 are decreased to a greater extent than pC99 in H4-BACE1-GFP cells depleted of UPS8 (Fig. 6, *B*, *D* and *E*).

Thus, we determined whether a decrease in BACE1 protein levels resulted in a decrease in Aβ formation in H4 cells expressing endogenous BACE1. We measured Aβ(1–40) content in conditioned media from H4 cells treated with USP8 or NT siRNA and found that there was a statistically significant decrease ($p = 0.002$) in Aβ(1–40) production with USP8 deple-

tion (Fig. 9). These data indicate that a decrease in BACE1 protein levels observed in USP8-depleted cells results in a corresponding decrease in Aβ formation.

Discussion

Previous investigators have shown that USP8 depletion leads to increased turnover of EGFR, a lysosome-degraded protein (23, 36, 37). We sought to determine whether USP8 depletion would lead to a similar decrease in BACE1 protein levels and a subsequent decrease in Aβ formation.

In our investigations, we found that USP8 depletion decreased levels of ectopically expressed BACE1-GFP, as well as endogenous BACE1 in H4 cells. USP8 depletion, however,
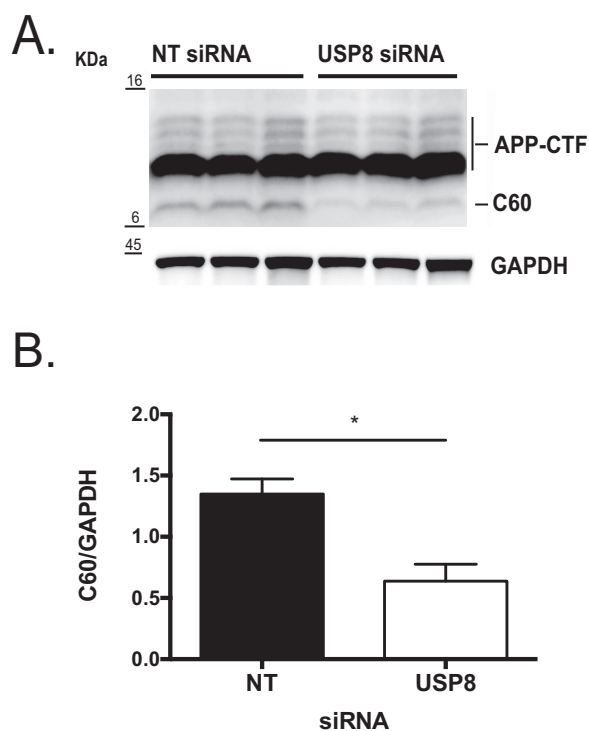
A.

B.

FIGURE 8. USP8 depletion decreases AICD protein levels. USP8 depletion decreases ectopically expressed AICD protein levels. APP-C60 was overexpressed in H4 cells by transient transfection. 24 post-transfection, cells were treated with USP8 or NT siRNA. *A,* representative Western blot; *B,* quantification of APP-C60 normalized to GAPDH. *Graphs* show mean and S.E.; $n = 3$ independent experiments; $p = 0.0187$; unpaired *t* test with Welch's correction. *NT,* non-targeting.
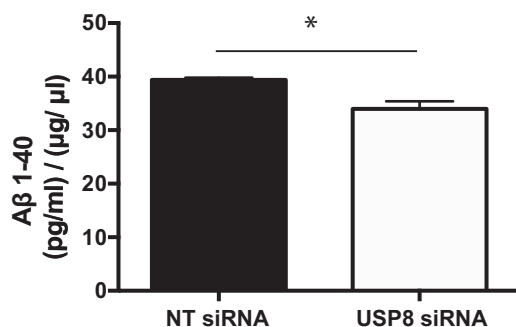

FIGURE 9. USP8 depletion decreases amyloid-β production in H4 cell line. Conditioned media was collected from H4 Naive cells treated with USP8 or NT siRNA. Aβ(1–40) in conditioned media was measured using ELISA kit. Aβ concentration (picograms/ml) was normalized to the protein concentration of cell lysates from the corresponding well (micrograms/μl). USP8 depletion reduced the amount of Aβ(1–40) in conditioned media collected for H4 naive cells. *Graph* shows mean and S.E.; $n = 8$–9 samples per condition from three independent experiments; *, $p = 0.002$, linear mixed model. *NT,* non-targeting.

did not affect ADAM10 and PS1 protein levels. This showed that USP8 depletion affected BACE1 but not other APP-cleaving proteins.

Given that BACE1-GFP cDNA transcription is regulated by the CMV promoter, the observed decrease in BACE1-GFP protein levels was unlikely due to changes in transcription or translation. Thus, we hypothesized that increased lysosomal degradation was likely responsible for decreased BACE1 protein levels in cells depleted of USP8. Accordingly, we found that treatment of USP8-depleted cells with chloroquine, a lysosomal

inhibitor, prevented BACE1 protein decrease. Furthermore, chloroquine treatment resulted in a similar accumulation of BACE1-GFP in both USP8-treated and NT-treated samples, demonstrating that lysosomal function is preserved when USP8 is depleted.

We hypothesized that an increase in BACE1 ubiquitination followed by increased lysosomal degradation was the mechanism for the BACE1 protein decrease. Accordingly, we found that USP8 depletion increased BACE1 ubiquitination at Lys-501. Moreover, we determined that USP8 directly deubiquitinated BACE1 in an *in vitro* cell-free assay. Together, these data showed that BACE1 is a direct substrate of USP8 deubiquitination, ruling out the possibility that USP8 was influencing BACE1 ubiquitination and protein levels indirectly, *e.g.* by deubiquitinating other DUBs and/or ubiquitin ligases. Currently, it is unknown whether USP8 deubiquitinates any other DUBs. However USP8 has been shown to deubiquitinate three E3 ligases, NRDP1 (48, 49), GRAIL (50), and Parkin (27). Furthermore, USP8 depletion is known to result in decreased STAM and HRS protein levels (24, 36). These two components of ESCRT0 are important for functional recruitment of ubiquitinated proteins to endosomes and for lysosomal degradation. However, an indirect effect of USP8 through these proteins is less likely, as it would lead to a decrease in BACE1 degradation and a resultant BACE1 accumulation, rather than the observed BACE1 protein decrease. Given that GGA3 is able to bind ubiquitinated cargoes and transfer them to the tumor susceptibility gene (TSG101), a ubiquitin-binding subunit of ESCRT complex I (51–54), functioning like HRS, it is possible that BACE1 is trafficked to the lysosomes by GGA3 even when levels of STAM are decreased in USP8-depleted cells.

Previous investigators have shown that USP8 depletion results in the accumulation of ubiquitinated proteins in the endosomes (24, 36, 41). We hypothesized that the decrease in BACE1 protein levels was a result of increased trafficking of BACE1 to the lysosomes and reduction of BACE1 in recycling endosomes, the intracellular site where BACE1 meets and processes APP (55–57). We found that USP8 depletion increased BACE1 localization in the early endosomes and the lysosomes, while decreasing BACE1 contained in the recycling endosomes. Furthermore, there was an increase in early and recycling endosome puncta size, although there was no change in lysosome size. Depletion of USP8 or overexpression of a dominant negative USP8 mutant has been shown to cause the accumulation of proteins within early endosomes and increase early endosome and MVB diameter. Furthermore, clustering of endosomes, facilitated by the formation of electron dense regions between endosomes, has been observed by electron microscopy (24, 41). These abnormalities have been attributed to numerous causes. First, it has been attributed to the accumulation of ubiquitinated proteins within endosomes (24, 34, 36, 41). Second, it has been attributed to the dysfunction of the endosomes due to loss of endosomal proteins like STAM and HRS (23, 36). Third, it has been suggested that USP8 is necessary for the promotion of lysosomal degradation, namely the need of USP8 to deubiquitinate proteins before they are finally transferred to the lysosomes (32). In our experiments, it is likely that there is an increased amount of ubiquitinated proteins within the early

endosomes. However, it is unlikely that there is a complete inhibition of protein transfer to the lysosomes, as the decrease in BACE1 protein suggests that there is successful protein degradation.

BACE1 is the rate-limiting enzyme in Aβ production. Because USP8 depletion resulted in a decrease in BACE1 protein levels, we expected a decrease in BACE1-mediated APP cleavage and also a decrease in Aβ formation. As expected, we found that USP8 depletion was accompanied by a decrease in the ratio of pC99 and pC89 to APP in H4-BACE1-GFP cells. pC99 and pC89 are phosphorylated forms of C99 and C89, direct products of BACE1-APP cleavage. Furthermore, USP8 depletion led to the decrease in pC99/APP, C99/APP, and pC89/APP in H4 cells, which did not overexpress BACE1. This demonstrated that the decrease in endogenous BACE1 after USP8 depletion was sufficient to decrease BACE1-mediated APP processing and that the effect was not limited to cells that overexpressed BACE1. Moreover, the decrease in BACE1-generated APP-CTF levels was likely due to a decrease in APP-CTF formation rather than a result of increased APP-CTF degradation, as USP8 depletion did not increase the degradation of overexpressed C99. This was important as APP CTFs can be ubiquitinated and are degraded in the lysosomes (43, 58). Furthermore, USP8 depletion decreased Aβ(1–40) production in H4 cells. This was consistent with the decrease in pC99 and C99 observed after USP8 depletion.

We also showed that USP8 depletion decreases ectopically expressed AICD protein levels, independent of decreases in APP-CTFs. Although AICD is known to be rapidly degraded in the cytoplasm (44), there is evidence to suggest that AICD may also be degraded in lysosomes, as drugs that prevent acidification of endosomes and lysosomes stabilize AICD levels (59). Furthermore, AICD is present in exosomes, which are derived from the intraluminal vesicles of MVBs or late endosomes, suggesting that AICD may be present within the endosome-lysosome system (60). The effect of USP8 depletion on C60 may be direct or indirect. The C60 sequence contains multiple lysine groups (61), which may be potential sites of ubiquitination. Moreover, the stability of AICD may be affected by changes in the stability of its binding partners. For example, the AICD is stabilized by binding to Fe65, an APP-binding adaptor protein (45). Fe65, a proteasomal degraded protein, is Lys-63 ubiquitinated (62, 63). Fe65 ubiquitination may be increased under conditions of USP8 depletion, as USP8 deubiquitinates Lys-63 chains. A resultant Fe65 decrease would account for a loss of AICD stability under conditions of USP8 depletion.

In summary, we found that depletion of USP8 decreases BACE1 protein levels by increasing BACE1 ubiquitination, decreasing the recycling of BACE1 while increasing its trafficking to the early endosome and lysosomes. As a consequence, BACE1-mediated APP processing and Aβ formation are decreased in USP8-depleted cells due not only to the decreased levels of BACE1 but also to reduced localization of BACE1 in the recycling endosomes where BACE1 meets and processes APP. Although the ubiquitin ligases involved in BACE1 ubiquitination at Lys-501 remain to be identified, our studies have identified USP8 as the DUB that directly deubiquinates BACE1 at Lys-501. Overexpression of ubiquitin C-terminal hydrolase

L1 (UCHL1) has been shown to decrease BACE1 protein levels, APP levels, and Aβ formation, whereas genetic and pharmacological inhibition of UCHL1 have been associated with an increase in BACE1 (64), most likely via activation of the NFκB pathway (64, 65). However, it has not been demonstrated whether the effect of UCHL1 is direct or indirect or whether its effect is due to its activity as a deubiquitinating enzyme or as a ligase, as it is believed to have dual roles (66).

BACE1 is a primary drug target for AD therapy. Phase II/III trials are currently ongoing for selective active site inhibitors of BACE1 (67). Although these drugs show initial promise for the treatment of AD, it remains unclear whether they will remain viable in future trials. As such, researching alternative methods of BACE1 inhibition remains highly important. An alternative approach to BACE1 small molecule inhibitors is the indirect inhibition of BACE1 through the modulation of regulatory mechanisms that control BACE1 levels or BACE1 trafficking to acidic compartments where it is optimally active. Thus, DUBs that when depleted result in a decrease in BACE1 represent an attractive pharmacological target for BACE1 inhibition. Several small molecule inhibitors for specific DUBs and screens to find such inhibitors have recently been developed (68–70). Our studies indicate that depletion of USP8 leads to decreased levels and activity of BACE1 and suggest that therapies able to accelerate BACE1 degradation (*e.g.* by increasing BACE1 ubiquitination) may represent a potential treatment for AD. The results of our studies aid not only our understanding of BACE1 degradation but also provide an alternative mechanism by which BACE1 and its product, Aβ, could be reduced.

Experimental Procedures

Antibodies and Expression Vectors—Antibodies used include the following: anti-GFP (Molecular Probes); anti-BACE1 (clone D10E5) (Cell Signaling); anti-GAPDH (Millipore); anti-USP8 (Cell Signaling); anti-FLAG (Sigma); anti-ADAM10 (Millipore); anti-ubiquitin (clone P4D1) (Santa Cruz Biotechnology); anti-PS1-N-terminal fragment (AB14), kindly provided by Dr. Samuel E. Gandy, Mount Sinai Hospital, New York; anti-LAMP2 (BD Biosciences); anti-EEA1 (BD Biosciences); anti-RAB11 (Cell Signaling); anti-APP-C-terminal fragment (clone C1/6.1) (Biolegend); and anti-β amyloid 1–16 (clone 6E10) (Biolegend). The BACE1-GFP expression vector was a gift from Dr. Tae Wan Kim, Columbia University, New York (71). The APP-C99 expression vector was a gift from Dr. Stefan Lichtenthaler, Technical University of Munich (TUM) School of Medicine, Munich, Germany (39). The APP-C60 plasmid was a gift from Dr. Dennis Selkoe, Brigham and Women's Hospital, Boston (45).

Site-directed Mutagenesis, BACE1-K501R-GFP Mutant— BACE1-GFP expression vector was subjected to site-directed mutagenesis using the QuikChange II site-directed mutagenesis kit (Agilent) according to the manufacturer's instructions. The mutation was introduced with the following primer (primer, 5′-GACATCTCCCTGCTGAGAAAGGGCAATTC-TGCAG-3′) (along with reverse complement primer). Mutagenesis was confirmed by DNA sequencing.

Generation of H4 Neuroglioma Stable Cell Lines Expressing BACE1-GFP and BACE1K501R-GFP—50,000 H4 neuroglioma cells were seeded in 6-well tissue culture plates (growth area, 9.6 cm², Falcon) and transiently transfected with 1.2 μg of BACE1-GFP or BACE1K501R-GFP expression vector. 24 h post-transfection, cells were transferred to a 150-mm Falcon tissue culture dish (growth area, 156.35 cm²). Cells were cultured in media containing 300 μg/ml G418 sulfate, geneticin (Calbiochem) for selection of colonies positive for expression vector. Isolated clones were screened for levels of BACE1 by fluorescence microscopy and Western blotting using rabbit anti-GFP antibody (Molecular Probes). Colonies were maintained using media containing 200 μg/ml G418 sulfate.

Generation of H4 Neuroglioma Stable Cell Lines Expressing APP-C99—125,000 H4 neuroglioma cells were seeded in 6-well tissue culture plates and were transiently transfected with 2 μg of APP-C99 expression vector. 48 h post-transfection, ~30,000 cells were sparsely plated in 150-mm Falcon tissue culture dishes. Cells were cultured in media containing 400 μg/ml hygromycin B (Invitrogen) for selection of colonies positive for expression vector. Colonies formed from surviving cells were screened by Western blotting for APP-C99 expression using anti-APP-C-terminal fragment (clone C1/6.1) (Biolegend) and anti-β amyloid 1–16 (clone 6E10) (Biolegend) antibodies. Colonies were maintained using media containing 200 μg/ml hygromycin B.

siRNA-mediated Knockdown of USP8—Reverse transfections were performed in 6-well tissue culture plates using Lipofectamine RNAiMAX transfection reagent (Invitrogen) and 25 nM siRNA. For reverse transfections, suspended cells were added to wells in which RNAi-Lipofectamine complexes were formed. Briefly, RNAi-Lipofectamine complexes were formed in wells using 6 μl of Lipofectamine RNAiMAX transfection reagent, 500 μl of Opti-MEM reduced serum media (Gibco), and human USP8#3 siRNA (Dharmacon; CUUCGUAAC-UUAGGAAAUA), human USP8#2 siRNA (Dharmacon; CCA-CUAGCAUCCACAAGUA), or NT siRNA pool (Dharmacon; UGGUUUACAUGUCGACUAA, UGGUUUACAUGUUGU-GUGA, UGGUUUACAUGUUUUCUGA, and UGGUUUA-CAUGUUUUCCUA). 400,000 H4-BACE1-GFP cells in 2 ml of antibiotic-free media were added to wells for a final volume of 2.5 ml. Cells were incubated at 37 °C and harvested 96 h post-transfection. Cells were lysed using radioimmunoprecipitation assay (RIPA) buffer (10 mM Tris, pH 8, 150 mM NaCl, 1% Nonidet P-40, 0.5% sodium deoxycholate, 0.1% SDS, 5 mM EDTA, 1% protease inhibitor mixture (ThermoScientific)). Cell lysates were analyzed using Western blotting.

Reverse transfections of H4 cells were performed using a final concentration of 5 nM siRNA. Initial trials using a concentration of 25 nM siRNA with this cell line resulted in cell toxicity. Thus, the siRNA concentration was reduced to 5 nM, and treatment time was reduced to 48 h. Briefly, 400,000 H4 cells were reverse transfected with 5 nM of human USP8#3 or NT siRNA. Cells were harvested 48 h post-transfection and lysed using RIPA buffer. Cell lysates were analyzed using Western blotting.

Transient Transfection of APP-C60—Two million H4 cells were seeded in 100 × 20-mm tissue culture dishes (growth area, 58.95 cm², Falcon) and were transiently transfected with

10 μg of C60 using Lipofectamine 2000 transfection reagent (Invitrogen). 24 h post-transfection, cells were trypsinized and reverse-transfected with 5 nM siRNA USP8 or NT siRNA in 6-well plates as described above. 48 h post-reverse transfection, samples were lysed with RIPA buffer, supplemented with 1% protease inhibitor mixture (ThermoScientific) and 5 mM 1,10-phenanthroline (Sigma).

Western Blot and Densitometry Analysis—Equal amounts of sample were separated by SDS-PAGE using 4–12% BisTris gels (ThermoFisher Scientific or Bio-Rad) and transferred to a PVDF membrane (Bio-Rad). Membranes were probed with the following antibodies: anti-GFP (Molecular Probes, 1:2000); anti-BACE1 (clone D10E5) (Cell Signaling, 1:1000); anti-GAPDH (Millipore, 1:2500); anti-USP8 (Cell Signaling, 1:1000); anti-FLAG (Sigma, 1:1000); anti-ADAM10 (Millipore, 1:1000); anti-ubiquitin (clone P4D1) (Santa Cruz Biotechnology, 1:1000); and anti-PS1-N-terminal fragment (AB14) (1:3000), kindly provided by Dr. S. Gandy. To detect full-length APP and APP-C-terminal fragments, equal amounts of each sample were separated by SDS-PAGE using 16.5% Tris-Tricine gels (Bio-Rad) and transferred to a PVDF membrane. Membranes were probed with anti-APP-C-terminal fragment (clone C1/6.1) antibody (Biolegend, 1:1000) or anti-β-amyloid 1–16 (clone 6E10) (Biolegend, 1:1000). Densitometry analysis was performed using an LAS-4000 Fuji Imaging System and Quantity One software (Bio-Rad). Protein levels were normalized to GAPDH levels, which served as a loading control given that no significant changes were observed in the levels of GAPDH in treated and untreated cells. Each sample was analyzed at least twice by Western blot. Each experiment included duplicate or triplicate samples for each treatment. At least three experiments were performed.

Lysosomal Inhibition of BACE1-GFP Cells—H4-BACE1-GFP cells were reverse-transfected with human USP8#3 or NT siRNA. 72 h post-transfection, cells were washed with Dulbecco's PBS (DPBS) and treated with media containing 25 μM chloroquine (Sigma) for ~16 h. Cells were washed with DPBS and lysed in RIPA buffer. BACE1-GPF protein levels in cell lysates were analyzed using Western blotting.

Immunoprecipitation of Ubiquitinated BACE1-GFP—H4-BACE1-GFP (or H4-BACEK501R) cells were reverse-transfected with human USP8#3 or NT siRNA. 96 h post-transfection, cells were washed with DPBS and lysed in immunoprecipitation lysis buffer (50 mM Tris-HCl, pH 7.4, 0.5 M NaCl, 1 mM EDTA, 1% Nonidet P-40, 10% glycerol, 5 mM 1,10-phenanthroline, 10 mM *N*-ethylmaleimide (NEM), 50 μM PR617 (Life Sensors)), and Protease Inhibitor mixture (ThermoScientific). Protein extracts were centrifuged at 14,000 rpm for 10 min. 200 μg of protein was precleared with 20 μl of equilibrated Protein A/G Plus-agarose beads (Santa Cruz Biotechnology) for 30 min at 4 °C. BACE1-GFP was immunoprecipitated from lysates using 5 μl of anti-GFP antibody (Molecular Probes) and 40 μl of protein A/G-agarose beads in 500 μl of immunoprecipitation lysis buffer overnight at 4 °C. Beads were washed with TBST, and proteins were eluted with 4× sample buffer, 3% β-mercaptoethanol for 10 min at 95 °C. Samples were separated by SDS-PAGE. Western blotting with an anti-ubiquitin antibody

(P4D1, Santa Cruz Biotechnology) was used to detect ubiquitinated BACE1.

Cell-free BACE1 Deubiquitination Assay—Ubiquitinated BACE1-GFP was immunoprecipitated with anti-GFP antibody and protein A/G plus-agarose beads from USP8-depleted samples, as described above. Beads were washed twice with TBST and once with DUB reaction buffer (50 mM Tris, pH 7.4, 1 mM DTT, 0.5 mM EDTA). Beads were split into three equal parts, combined with 0.5 μM human recombinant FLAG-USP8 (BPS Bioscience) in 50 μl of DUB reaction buffer and incubated at 37 °C for 120 min with shaking. 5 mM (NEM), a cysteine protease inhibitor that inhibits DUBs, was included in some reactions. Reaction was stopped by adding 4× sample buffer, 3% β-mercaptoethanol, and incubation at 95 °C for 10 min. Samples were separated by SDS-PAGE, and BACE1 ubiquitination levels were evaluated using Western blotting.

Immunocytochemistry—H4 BACE1-GFP cells were transfected with USP8 siRNA or non-targeting siRNA. 96 h post-transfection, cells were washed with DPBS and fixed with 4% formaldehyde in DPBS for 15 min at room temperature. Coverslips were washed twice with 0.1 M glycine in DPBS and then cells were permeabilized with 0.1% Triton X-100 in DPBS for 5 min. Coverslips were blocked with 5% BSA in DPBS and incubated overnight at 4 °C with primary antibody. Late endosomes/lysosomes and early endosomes were labeled with monoclonal antibodies against LAMP2 (1:800; BD Biosciences) and EEA1 (1:800; BD Biosciences), respectively. Recycling endosomes were labeled with antibodies against RAB11 (1:400; Cell Signaling). Coverslips were incubated in secondary antibody, goat anti-mouse, or anti-rabbit Alexa Fluor 568 (Molecular Probes; 1:500) for 1 h at room temperature. Coverslips were incubated in DAPI dilactate (1:10,000) for 5 min. Coverslips were mounted onto slides using Fluoromount-G (Southern Biotech). Images were acquired with a Nikon Eclipse T*i* inverted microscope, equipped with a Nikon A1R+ confocal system, and a Nikon Plan Apo VC 60× oil/1.4 numerical aperture objective (1024 × 1024 resolution). Images were acquired using NIS Elements software (Nikon). Z-stack projections thorough cells were acquired taking 0.5 μM steps. Images were analyzed using a custom macro on ImageJ. Briefly, the sum of the slices was generated. Background subtraction (rolling ball radius = 20), median filter (radius = 1), and triangle threshold were applied to images with BACE1, EEA1, RAB11, and LAMP2 labeling to delineate regions positive for labeling. Percentage of BACE1 in the early endosome was determined by finding the quotient of the total GFP intensity in EEA1-positive regions and the total GFP intensity within the cell. Percentage of BACE1-GFP in lysosomes and recycling endosomes was calculated in a similar manner using LAMP2-positive and RAB11-positive regions, respectively.

Amyloid-β ELISA—Conditioned media were collected from H4-BACE1-GFP and H4 cells treated with USP8 or NT siRNA. 72 h post-transfection (H4-BACE1-GFP) or 24 h post-transfection (H4 Naive), media were removed and replaced with 0.8 ml of fresh media. 24 h later, the media were collected. Media were centrifuged immediately after collection for 10 min at 10,000 × *g* to remove cellular debris. Cells were also harvested for Western blotting analysis. Aβ(1–40) was measured using a human amyloid-β(1–40) ELISA kit (ThermoFisher Scientific). Aβ concentration in media (picograms/ml) was normalized to the protein concentration of cell lysates from the corresponding well (micrograms/μl).

Statistical Analysis—Statistical analysis was performed using Prism 6 (GraphPad software). The means of samples were compared using either one-way analysis of variance or the unpaired *t* test with Welch's correction. Values were expressed as mean and standard error of the mean. The α level was set as 0.05. ELISA data were analyzed using IBM SPSS, version 22 (IBM). Samples were compared using a linear mixed effect model, where the fixed effect was siRNA treatment (USP8 or NT), and the random effect was each independent experiment. Sample size (*n*) was each individual sample.

References

1. Sinha, S., Anderson, J. P., Barbour, R., Basi, G. S., Caccavello, R., Davis, D., Doan, M., Dovey, H. F., Frigon, N., Hong, J., Jacobson-Croak, K., Jewett, N., Keim, P., Knops, J., Lieberburg, I., *et al.* (1999) Purification and cloning of amyloid precursor protein β-secretase from human brain. *Nature* **402,** 537–540
2. Yan, R., Bienkowski, M. J., Shuck, M. E., Miao, H., Tory, M. C., Pauley, A. M., Brashier, J. R., Stratman, N. C., Mathews, W. R., Buhl, A. E., Carter, D. B., Tomasselli, A. G., Parodi, L. A., Heinrikson, R. L., and Gurney, M. E. (1999) Membrane-anchored aspartyl protease with Alzheimer's disease β-secretase activity. *Nature* **402,** 533–537
3. Hong, L., Koelsch, G., Lin, X., Wu, S., Terzyan, S., Ghosh, A. K., Zhang, X. C., and Tang, J. (2000) Structure of the protease domain of memapsin 2 (β-secretase) complexed with inhibitor. *Science* **290,** 150–153
4. Vassar, R., Bennett, B. D., Babu-Khan, S., Kahn, S., Mendiaz, E. A., Denis, P., Teplow, D. B., Ross, S., Amarante, P., Loeloff, R., Luo, Y., Fisher, S., Fuller, J., Edenson, S., Lile, J., *et al.* (1999) β-Secretase cleavage of Alzheimer's amyloid precursor protein by the transmembrane aspartic protease BACE. *Science* **286,** 735–741
5. De Strooper, B. (2000) Alzheimer's disease. Closing in on γ-secretase. *Nature* **405,** 627, 629
6. Buxbaum, J. D., Liu, K. N., Luo, Y., Slack, J. L., Stocking, K. L., Peschon, J. J., Johnson, R. S., Castner, B. J., Cerretti, D. P., and Black, R. A. (1998) Evidence that tumor necrosis factor α converting enzyme is involved in regulated α-secretase cleavage of the Alzheimer amyloid protein precursor. *J. Biol. Chem.* **273,** 27765–27767
7. Lammich, S., Kojro, E., Postina, R., Gilbert, S., Pfeiffer, R., Jasionowski, M., Haass, C., and Fahrenholz, F. (1999) Constitutive and regulated α-secretase cleavage of Alzheimer's amyloid precursor protein by a disintegrin metalloprotease. *Proc. Natl. Acad. Sci. U.S.A.* **96,** 3922–3927
8. Haass, C. (2004) Take five-BACE and the γ-secretase quartet conduct Alzheimer's amyloid β-peptide generation. *EMBO J.* **23,** 483–488
9. Lichtenthaler, S. F., Haass, C., and Steiner, H. (2011) Regulated intramembrane proteolysis–lessons from amyloid precursor protein processing. *J. Neurochem.* **117,** 779–796
10. Citron, M. (2004) β-Secretase inhibition for the treatment of Alzheimer's

disease–promise and challenge. *Trends Pharmacol. Sci.* **25,** 92–97

11. Haass, C., Kaether, C., Thinakaran, G., and Sisodia, S. (2012) Trafficking and proteolytic processing of APP. *Cold Spring Harb. Perspect. Med.* **2,** a006270

12. Bonifacino, J. S., and Traub, L. M. (2003) Signals for sorting of transmembrane proteins to endosomes and lysosomes. *Annu. Rev. Biochem.* **72,** 395– 447

13. Koh, Y. H., von Arnim, C. A., Hyman, B. T., Tanzi, R. E., and Tesco, G. (2005) BACE is degraded via the lysosomal pathway. *J. Biol. Chem.* **280,** 32499 –32504

14. Tesco, G., Koh, Y. H., Kang, E. L., Cameron, A. N., Das, S., Sena-Esteves, M., Hiltunen, M., Yang, S.-H., Zhong, Z., Shen, Y., Simpkins, J. W., and Tanzi, R. E. (2007) Depletion of gga3 stabilizes BACE and enhances β-secretase activity. *Neuron* **54,** 721–737

15. Walker, K. R., Kang, E. L., Whalen, M. J., Shen, Y., and Tesco, G. (2012) Depletion of gga1 and gga3 mediates postinjury elevation of BACE1. *J. Neurosci.* **32,** 10423–10437

16. Kang, E. L., Cameron, A. N., Piazza, F., Walker, K. R., and Tesco, G. (2010) Ubiquitin regulates gga3-mediated degradation of BACE1. *J. Biol. Chem.* **285,** 24108 –24119

17. Kang, E. L., Biscaro, B., Piazza, F., and Tesco, G. (2012) BACE1 protein endocytosis and trafficking are differentially regulated by ubiquitination at lysine 501 and the di-leucine motif in the carboxyl terminus. *J. Biol. Chem.* **287,** 42867– 42880

18. Piper, R. C., and Luzio, J. P. (2007) Ubiquitin-dependent sorting of integral membrane proteins for degradation in lysosomes. *Curr. Opin. Cell Biol.* **19,** 459– 465

19. Davies, B. A., Lee, J. R., Oestreich, A. J., and Katzmann, D. J. (2009) Membrane protein targeting to the MVB/lysosome. *Chem. Rev.* **109,** 1575–1586

20. Lauwers, E., Erpapazoglou, Z., Haguenauer-Tsapis, R., and André, B. (2010) The ubiquitin code of yeast permease trafficking. *Trends Cell Biol.* **20,** 196 –204

21. Clague, M. J., Coulson, J. M., and Urbé, S. (2012) Cellular functions of the dubs. *J. Cell Sci.* **125,** 277–286

22. Bruzzone, F., Vallarino, M., Berruti, G., and Angelini, C. (2008) Expression of the deubiquitinating enzyme mubpy in the mouse brain. *Brain Res.* **1195,** 56 – 66

23. Mizuno, E., Iura, T., Mukai, A., Yoshimori, T., Kitamura, N., and Komada, M. (2005) Regulation of epidermal growth factor receptor down-regulation by ubpy-mediated deubiquitination at endosomes. *Mol. Biol. Cell* **16,** 5163–5174

24. Row, P. E., Prior, I. A., McCullough, J., Clague, M. J., and Urbé, S. (2006) The ubiquitin isopeptidase ubpy regulates endosomal ubiquitin dynamics and is essential for receptor down-regulation. *J. Biol. Chem.* **281,** 12618 –12624

25. Ceriani, M., Amigoni, L., D'Aloia, A., Berruti, G., and Martegani, E. (2015) The deubiquitinating enzyme ubpy/usp8 interacts with trka and inhibits neuronal differentiation in pc12 cells. *Exp. Cell Res.* **333,** 49 –59

26. Clague, M. J., and Urbé, S. (2006) Endocytosis: The dub version. *Trends Cell Biol.* **16,** 551–559

27. Durcan, T. M., Tang, M. Y., Pérusse, J. R., Dashti, E. A., Aguileta, M. A., McLelland, G. L., Gros, P., Shaler, T. A., Faubert, D., Coulombe, B., and Fon, E. A. (2014) Usp8 regulates mitophagy by removing k6-linked ubiquitin conjugates from parkin. *EMBO J.* **33,** 2473–2491

28. Alwan, H. A., and van Leeuwen, J. E. (2007) Ubpy-mediated epidermal growth factor receptor (egfr) de-ubiquitination promotes egfr degradation. *J. Biol. Chem.* **282,** 1658 –1669

29. Sirisaengtaksin, N., Gireud, M., Yan, Q., Kubota, Y., Meza, D., Waymire, J. C., Zage, P. E., and Bean, A. J. (2014) Ube4b protein couples ubiquitination and sorting machineries to enable epidermal growth factor receptor (egfr) degradation. *J. Biol. Chem.* **289,** 3026 –3039

30. Scudder, S. L., Goo, M. S., Cartier, A. E., Molteni, A., Schwarz, L. A., Wright, R., and Patrick, G. N. (2014) Synaptic strength is bidirectionally controlled by opposing activity-dependent regulation of nedd4-1 and usp8. *J. Neurosci.* **34,** 16637–16649

31. Smith, G. A., Fearnley, G. W., Abdul-Zani, I., Wheatcroft, S. B., Tomlinson, D. C., Harrison, M. A., and Ponnambalam, S. (2016) Vegfr2 trafficking, signaling and proteolysis is regulated by the ubiquitin isopeptidase usp8. *Traffic* **17,** 53– 65

32. Oh, Y. M., Lee, S. B., Choi, J., Suh, H. Y., Shim, S., Song, Y. J., Kim, B., Lee, J. M., Oh, S. J., Jeong, Y., Cheong, K. H., Song, P. H., and Kim, K. A. (2014) Usp8 modulates ubiquitination of lrig1 for met degradation. *Sci. Rep.* **4,** 4980

33. Balut, C. M., Loch, C. M., and Devor, D. C. (2011) Role of ubiquitylation and usp8-dependent deubiquitylation in the endocytosis and lysosomal targeting of plasma membrane kca3.1. *FASEB J.* **25,** 3938 –3948

34. Hasdemir, B., Murphy, J. E., Cottrell, G. S., and Bunnett, N. W. (2009) Endosomal deubiquitinating enzymes control ubiquitination and down-regulation of protease-activated receptor 2. *J. Biol. Chem.* **284,** 28453–28466

35. Hislop, J. N., Henry, A. G., Marchese, A., and von Zastrow, M. (2009) Ubiquitination regulates proteolytic processing of g protein-coupled receptors after their sorting to lysosomes. *J. Biol. Chem.* **284,** 19361–19370

36. Niendorf, S., Oksche, A., Kisser, A., Löhler, J., Prinz, M., Schorle, H., Feller, S., Lewitzky, M., Horak, I., and Knobeloch, K.-P. (2007) Essential role of ubiquitin-specific protease 8 for receptor tyrosine kinase stability and endocytic trafficking *in vivo*. *Mol. Cell. Biol.* **27,** 5029 –5039

37. Berlin, I., Schwartz, H., and Nash, P. (2010) Regulation of epidermal growth factor receptor ubiquitination and trafficking by the usp8: Stam complex. *J. Biol. Chem.* **285,** 34909 –34921

38. Kato, M., Miyazawa, K., and Kitamura, N. (2000) A deubiquitinating enzyme ubpy interacts with the src homology 3 domain of hrs-binding protein via a novel binding motif px(v/i)(d/n)rxxkp. *J. Biol. Chem.* **275,** 37481–37487

39. Lichtenthaler, S. F., Ida, N., Multhaup, G., Masters, C. L., and Beyreuther, K. (1997) Mutations in the transmembrane domain of app altering γ-secretase specificity. *Biochemistry* **36,** 15396 –15403

40. Bache, K. G., Raiborg, C., Mehlum, A., and Stenmark, H. (2003) Stam and hrs are subunits of a multivalent ubiquitin-binding complex on early endosomes. *J. Biol. Chem.* **278,** 12513–12521

41. Mizuno, E., Kobayashi, K., Yamamoto, A., Kitamura, N., and Komada, M. (2006) A deubiquitinating enzyme ubpy regulates the level of protein ubiquitination on endosomes. *Traffic* **7,** 1017–1031

42. Bowers, K., Piper, S. C., Edeling, M. A., Gray, S. R., Owen, D. J., Lehner, P. J., and Luzio, J. P. (2006) Degradation of endocytosed epidermal growth factor and virally ubiquitinated major histocompatibility complex class i is independent of mammalian escrtii. *J. Biol. Chem.* **281,** 5094 –5105

43. Morel, E., Chamoun, Z., Lasiecka, Z. M., Chan, R. B., Williamson, R. L., Vetanovetz, C., Dall'Armi, C., Simoes, S., Point Du Jour, K. S., McCabe, B. D., Small, S. A., and Di Paolo, G. (2013) Phosphatidylinositol-3-phosphate regulates sorting and processing of amyloid precursor protein through the endosomal system. *Nat. Commun.* **4,** 2250

44. Edbauer, D., Winkler, E., Haass, C., and Steiner, H. (2002) Presenilin and nicastrin regulate each other and determine amyloid β-peptide production via complex formation. *Proc. Natl. Acad. Sci. U.S.A.* **99,** 8666 – 8671

45. Kimberly, W. T., Zheng, J. B., Guénette, S. Y., and Selkoe, D. J. (2001) The intracellular domain of the β-amyloid precursor protein is stabilized by fe65 and translocates to the nucleus in a notch-like manner. *J. Biol. Chem.* **276,** 40288 – 40292

46. Urbé, S., Liu, H., Hayes, S. D., Heride, C., Rigden, D. J., and Clague, M. J. (2012) Systematic survey of deubiquitinase localization identifies usp21 as a regulator of centrosome- and microtubule-associated functions. *Mol. Biol. Cell* **23,** 1095–1103

47. Creemers, J. W., Ines Dominguez, D., Plets, E., Serneels, L., Taylor, N. A., Multhaup, G., Craessaerts, K., Annaert, W., and De Strooper, B. (2001) Processing of β-secretase by furin and other members of the proprotein convertase family. *J. Biol. Chem.* **276,** 4211– 4217

48. Wu, X., Yen, L., Irwin, L., Sweeney, C., and Carraway, K. L., 3rd. (2004) Stabilization of the e3 ubiquitin ligase nrdp1 by the deubiquitinating enzyme usp8. *Mol. Cell. Biol.* **24,** 7748 –7757

49. Avvakumov, G. V., Walker, J. R., Xue, S., Finerty, P. J., Jr., Mackenzie, F., Newman, E. M., and Dhe-Paganon, S. (2006) Amino-terminal dimerization, nrdp1-rhodanese interaction, and inhibited catalytic domain conformation of the ubiquitin-specific protease 8 (usp8). *J. Biol. Chem.* **281,** 38061–38070

50. Soares, L., Seroogy, C., Skrenta, H., Anandasabapathy, N., Lovelace, P., Chung, C. D., Engleman, E., and Fathman, C. G. (2004) Two isoforms of otubain 1 regulate t cell anergy via grail. *Nat. Immunol.* **5,** 45–54

51. Puertollano, R., and Bonifacino, J. S. (2004) Interactions of gga3 with the ubiquitin sorting machinery. *Nat. Cell Biol.* **6,** 244–251

52. Bilodeau, P. S., Winistorfer, S. C., Allaman, M. M., Surendhran, K., Kearney, W. R., Robertson, A. D., and Piper, R. C. (2004) The gat domains of clathrin-associated gga proteins have two ubiquitin binding motifs. *J. Biol. Chem.* **279,** 54808–54816

53. Prag, G., Lee, S., Mattera, R., Arighi, C. N., Beach, B. M., Bonifacino, J. S., and Hurley, J. H. (2005) Structural mechanism for ubiquitinated-cargo recognition by the golgi-localized, γ-ear-containing, adp-ribosylation-factor-binding proteins. *Proc. Natl. Acad. Sci. U.S.A.* **102,** 2334–2339

54. Kawasaki, M., Shiba, T., Shiba, Y., Yamaguchi, Y., Matsugaki, N., Igarashi, N., Suzuki, M., Kato, R., Kato, K., Nakayama, K., and Wakatsuki, S. (2005) Molecular mechanism of ubiquitin recognition by gga3 gat domain. *Genes Cells* **10,** 639–654

55. Das, U., Wang, L., Ganguly, A., Saikia, J. M., Wagner, S. L., Koo, E. H., and Roy, S. (2016) Visualizing app and bace-1 approximation in neurons yields insight into the amyloidogenic pathway. *Nat. Neurosci.* **19,** 55–64

56. Das, U., Scott, D. A., Ganguly, A., Koo, E. H., Tang, Y., and Roy, S. (2013) Activity-induced convergence of app and bace-1 in acidic microdomains via an endocytosis-dependent pathway. *Neuron* **79,** 447–460

57. Buggia-Prévot, V., Fernandez, C. G., Udayar, V., Vetrivel, K. S., Elie, A., Roseman, J., Sasse, V. A., Lefkow, M., Meckler, X., Bhattacharyya, S., George, M., Kar, S., Bindokas, V. P., Parent, A. T., Rajendran, L., *et al.* (2013) A function for ehd family proteins in unidirectional retrograde dendritic transport of bace1 and Alzheimer's disease Aβ production. *Cell Rep.* **5,** 1552–1563

58. Bustamante, H. A., Rivera-Dictter, A., Cavieres, V. A., Muñoz, V. C., González, A., Lin, Y., Mardones, G. A., and Burgos, P. V. (2013) Turnover of c99 is controlled by a crosstalk between erad and ubiquitin-independent lysosomal degradation in human neuroglioma cells. *PLoS ONE* **8,** e83096

59. Vingtdeux, V., Hamdane, M., Bégard, S., Loyens, A., Delacourte, A., Beauvillain, J. C., Buée, L., Marambaud, P., and Sergeant, N. (2007) Intracellular pH regulates amyloid precursor protein intracellular domain accumulation. *Neurobiol. Dis.* **25,** 686–696

60. Vingtdeux, V., Hamdane, M., Loyens, A., Gelé, P., Drobeck, H., Bégard, S., Galas, M. C., Delacourte, A., Beauvillain, J. C., Buée, L., and Sergeant, N. (2007) Alkalizing drugs induce accumulation of amyloid precursor protein by-products in luminal vesicles of multivesicular bodies. *J. Biol. Chem.* **282,** 18197–18205

61. Slomnicki, L. P., and Lesniak, W. (2008) A putative role of the amyloid precursor protein intracellular domain (aicd) in transcription. *Acta Neurobiol. Exp.* **68,** 219–228

62. Lee, E. J., Hyun, S., Chun, J., Shin, S. H., and Kang, S. S. (2009) Ubiquitylation of fe65 adaptor protein by neuronal precursor cell expressed developmentally down regulated 4–2 (nedd4-2) via the ww domain interaction with fe65. *Exp. Mol. Med.* **41,** 555–568

63. Matz, A., Lee, S. J., Schwedhelm-Domeyer, N., Zanini, D., Holubowska, A., Kannan, M., Farnworth, M., Jahn, O., Göpfert, M. C., and Stegmüller, J. (2015) Regulation of neuronal survival and morphology by the e3 ubiquitin ligase rnf157. *Cell Death Differ.* **22,** 626–642

64. Zhang, M., Deng, Y., Luo, Y., Zhang, S., Zou, H., Cai, F., Wada, K., and Song, W. (2012) Control of bace1 degradation and app processing by ubiquitin carboxyl-terminal hydrolase l1. *J. Neurochem.* **120,** 1129–1138

65. Guglielmotto, M., Monteleone, D., Boido, M., Piras, A., Giliberto, L., Borghi, R., Vercelli, A., Fornaro, M., Tabaton, M., and Tamagno, E. (2012) Aβ1–42-mediated down-regulation of uch-l1 is dependent on NF-κB activation and impaired bace1 lysosomal degradation. *Aging Cell* **11,** 834–844

66. Liu, Y., Fallon, L., Lashuel, H. A., Liu, Z., and Lansbury, P. T., Jr. (2002) The uch-l1 gene encodes two opposing enzymatic activities that affect α-synuclein degradation and parkinson's disease susceptibility. *Cell* **111,** 209–218

67. Vassar, R., Kuhn, P. H., Haass, C., Kennedy, M. E., Rajendran, L., Wong, P. C., and Lichtenthaler, S. F. (2014) Function, therapeutic potential and cell biology of BACE proteases: current status and future prospects. *J. Neurochem.* **130,** 4–28

68. Chauhan, D., Tian, Z., Nicholson, B., Kumar, K. G., Zhou, B., Carrasco, R., McDermott, J. L., Leach, C. A., Fulcinniti, M., Kodrasov, M. P., Weinstock, J., Kingsbury, W. D., Hideshima, T., Shah, P. K., Minvielle, S., *et al.* (2012) A small molecule inhibitor of ubiquitin-specific protease-7 induces apoptosis in multiple myeloma cells and overcomes bortezomib resistance. *Cancer Cell* **22,** 345–358

69. Weinstock, J., Wu, J., Cao, P., Kingsbury, W. D., McDermott, J. L., Kodrasov, M. P., McKelvey, D. M., Suresh Kumar, K. G., Goldenberg, S. J., Mattern, M. R., and Nicholson, B. (2012) Selective dual inhibitors of the cancer-related deubiquitylating proteases usp7 and usp47. *ACS Med. Chem. Lett.* **3,** 789–792

70. Arnst, J. L., Davies, C. W., Raja, S. M., Das, C., and Natarajan, A. (2013) High-throughput compatible fluorescence resonance energy transfer-based assay to identify small molecule inhibitors of amsh deubiquitinase activity. *Anal. Biochem.* **440,** 71–77

71. Finan, G. M., Okada, H., and Kim, T. W. (2011) Bace1 retrograde trafficking is uniquely regulated by the cytoplasmic domain of sortilin. *J. Biol. Chem.* **286,** 12602–12616